Article title

Uncertainty determination in high-temperature spectral emissivity measurement method of coatings

Authors

Petra Honnerová, Jiří Martan, Milan Honner

Keywords

direct measurement, optical properties, spectral emissivity, uncertainty, high temperature

Abstract

The paper deals with uncertainty analyses of the new laboratory method for the measurement of spectral emissivity of high-temperature coatings. These coatings are intended to increase heat transfer in various industrial applications. The experimental set-up of the method is shortly introduced. The method is innovative in the application of scanning laser heating and in the coating surface temperature measurement using an infrared camera with a reference coating. Methods for total and partial uncertainty evaluation are described. As the uncertainty is always related to individual sample being measured, the DupliColor 800°C paint (MOTIP Dupli Ltd.) is used as an example to introduce the results. Except the absorption bands the uncertainty is below 4 % with coverage factor $k = 2$. Uncertainty spectral and temperature dependences are analyzed. Contribution of individual uncertainty sources as measured sample signal, measured laboratory blackbody signal, sample surface temperature, laboratory blackbody temperature, surroundings temperature, blackbody effective emissivity and surroundings emissivity and their sub-components are discussed.

Nomenclature

L	radiance
R	response function
T	temperature
V	spectrometer signal
X	individual source
Y	sub-component

Greek Symbols

Δ	difference
ε	emissivity
λ	wavelength
μ	absolute uncertainty
υ	wave number
ξ	relative uncertainty

Subscripts or superscripts

$\wedge$	effective value
0	surroundings
1	lower value
2	higher value
B	blackbody
i	summing index of individual sources
j	summing index of sub-components
λ	spectral dependence
max	maximum
ref	reference
S	sample
t	time dependence

1. Introduction

Spectral emissivity describes the ability of material surface to emit radiation on a certain wavelength in relation to the radiation of a blackbody. It is the basic material property characterizing radiation heat transfer. The emissivity influence of processes and efficiency of high-temperature energy conversion devices is substantial. It concerns research of furnaces [1 – 3], heat exchangers [4, 5], combustors [6], solar heat collectors [7], thermal energy storage [8], electric heaters [9], etc.

The research of applications of various materials in these devices brings about requirements for the development of laboratory methods for emissivity analyses to measure temperature and wavelength dependences. The spectral emissivity radiometric measurement methods were developed in various laboratory arrangements [10, 11]. The methods differ in the applied reference sources of radiation, systems of sample clamping and heating, detection systems, methods for the determination of surface temperature, and procedures for emissivity evaluation. Emissivity spectral distribution together with the uncertainty estimation is the required output of the methods. Therefore uncertainty analyses and discussions on error sources are usually published side by the introduction of the newly developed emissivity measurement method or by its application.

Theoretically the problems of uncertainty determination concerning the emissivity measurement are discussed in [12]. The influences of surrounding/sample area ratio, surroundings emissivity, dependences on wavelength, sample surface temperature or surroundings temperature are analyzed in this paper. On contrary the published papers [13 – 19] introduce the experimental set-up and show uncertainty evaluations in relation to the specific method arrangement.

A new experimental set-up for the spectral emissivity high-temperature analyses has been developed at the New Technologies Research Centre at the University of West Bohemia in Pilsen [20]. The method is intended to measure thick coating samples; however bulk metallic or ceramic samples can be analyzed as well. The method is innovative in the application of scanning laser heating [21] and in the coating surface temperature measurement using an infrared camera with a reference coating. Advantages of the heating method include the possibility to uniformly heat various samples concerning their magnitude and shape and the high heating rate on the required temperature level.

The advantages of the applied surface temperature measurement technique are the ability to consider temperature drop on the analyzed coating, the ability to monitor the temperature field of the sample and the non-contact principle without the installation and calibration of contact sensors. This paper is dealing with in-depth uncertainty determination concerning the method.

Some of the uncertainty aspects have been already mentioned in the paper [20] however very briefly. Our motivation is to introduce details throughout this paper that could be available to the heat transfer community and to the readers of our further research papers with applications of the emissivity measurement method and with results of analyses of various high-temperature materials for industrial applications. Therefore the influence of the most important parameters as the measured

signals of the sample and laboratory blackbody, temperatures of the sample surface, blackbody and surroundings and emissivity of blackbody and surroundings is introduced in this paper. Results are shown in the form of spectral and temperature uncertainty dependences. The contribution of individual sources of uncertainty and their sub-components to the overall uncertainty is analyzed.

2. Experimental system and emissivity evaluation

The experimental system for spectral emissivity measurement uses a direct method of comparison of radiation fluxes from the sample and reference blackbody at the same temperature. The system consists of a FTIR spectrometer, heating laser, sample, reference blackbody, infrared camera, optical apertures, shutter, pointing lasers, rotary mirror and cover box [20]. The radiation sources are the heated sample and reference high temperature blackbody. The rotary mirror chooses the source of radiation. The spectrometer is used for detection of radiation and spectral resolution. The optical apertures define the spot of emissivity measurement on sample. The infrared camera precisely measures temperature on the surface of the measured coating. The spectrometer uses KBr beam splitter and temperature stabilized DTGS detector. The detected spectral range is 1.38 – 26 μm.

The sample is heated by a 400 W continuous fiber laser with scan head. The scan head directs the laser beam on predefined paths on the back side of the sample in order to produce homogeneous temperature distribution on the front side [21]. The laser heating enables fast heating and temperature stabilization on different temperature levels and also measurement of samples with different size and shape. The temperature range of the system is 250 to 1000°C.

The sample temperature measurement by the IR camera uses a reference coating deposited on a half of the sample over the measured coating [20, 22]. The emissivity of the reference coating is once precisely calibrated with the infrared camera using a thermocouple under the coating in order to determine temperature on the surface of the measured coating. Further measurements are done without contact. The sample temperature homogeneity enables supposition of the same temperature in two symmetrical positions on the sample: the spot for temperature measurement by infrared camera and the spot for emissivity measurement by spectrometer.

The normal spectral emissivity of the measured coating $\varepsilon_{\lambda,n}(\lambda,T)$ is calculated according to [20]

$$\varepsilon_{\lambda,n}(\lambda,T)=\frac{V_\lambda^S\left(\lambda,T^S\right)-V_\lambda^{B1}\left(\lambda,T^{B1}\right)}{V_\lambda^{B2}\left(\lambda,T^{B2}\right)-V_\lambda^{B1}\left(\lambda,T^{B1}\right)}\cdot\frac{\hat{\varepsilon}^B L_\lambda^{B2}\left(\lambda,T^{B2}\right)-\hat{\varepsilon}^B L_\lambda^{B1}\left(\lambda,T^{B1}\right)}{L_\lambda^B\left(\lambda,T^S\right)-\varepsilon^0 L_\lambda^B\left(\lambda,T^0\right)}+ \\ +\frac{\hat{\varepsilon}^B L_\lambda^{B1}\left(\lambda,T^{B1}\right)-\varepsilon^0 L_\lambda^B\left(\lambda,T^0\right)}{L_\lambda^B\left(\lambda,T^S\right)-\varepsilon^0 L_\lambda^B\left(\lambda,T^0\right)}, \quad (1)$$

where λ is wavelength, T temperature, V spectrometer signal, L^B_λ blackbody spectral radiance, ε emissivity, $\hat{\varepsilon}^B$ blackbody effective emissivity, indexes *B1* and *B2* mean blackbody at lower and higher temperatures, index *S* means investigated sample and index *0* means surroundings. The spectrometer signals are obtained by measurement of radiation of sample at sample temperature and

blackbody at higher and lower temperatures around the sample temperature. The blackbody spectral radiances are computed according to the Planck's law at specified temperatures.

3. Method for total uncertainty evaluation

Spectral dependence of normal emissivity of each measured coating is loaded by an uncertainty that coming out from the used measuring apparatus, and the chosen method of measurement and evaluation of emissivity. In this method, the total uncertainty of spectral normal emissivity $\mu(\varepsilon_{\lambda,n})$ is evaluated according to [23 – 25] as a combined standard uncertainty given by the equation

$$\mu(\varepsilon_{\lambda,n}) = \left[\sum_{i=1}^{n} \left(\frac{\partial \varepsilon_{\lambda,n}}{\partial X_i} \cdot \mu(X_i) \right)^2 \right]^{1/2} , \tag{2}$$

where X_i are the individual sources of uncertainty, $\mu(X_i)$ the absolute partial uncertainties of individual sources, $\partial \varepsilon_{\lambda,n} / \partial X_i$ the respective sensitivity coefficients, and $\left[\left(\partial \varepsilon_{\lambda,n} / \partial X_i \right) \cdot \mu(X_i) \right]$ are individual contributions of absolute partial uncertainty to total uncertainty of emissivity. The individual sources of uncertainty include all variables in equation (1). Summary of the individual sources of uncertainties is shown in Table 1.

Each absolute partial uncertainty of individual source is determined from sub-components Y_j as the product of individual sources of uncertainty X_i and relative partial uncertainties of individual sources $\xi(X_i)$ according to equation

$$\mu(X_i) = X_i \cdot \xi(X_i) , \tag{3}$$

where

$$\xi(X_i) = \left[\sum_{j=1}^{m} \left(\xi(Y_j) \right)^2 \right]^{1/2} , \tag{4}$$

and where $\xi(Y_j)$ are the relative partial uncertainties of sub-components. The equations (3, 4) are simplification of equation (2) for the case of multiplication of sub-components in a component. Because the real sensitivity coefficients are not known, this simplification is used. The groups of sub-components are also shown in Table 1 including the type of uncertainty and discussed in detail in the following section.

Table 1.

Summary of individual sources of uncertainties and groups of sub-components included in the total uncertainty of spectral normal emissivity of coatings. The uncertainties of type A are determined from the results of repeated measurements by the statistical analysis of a series of the measured values. The uncertainties of type B are evaluated by other means than the statistical analysis of a series of the measured values.

Individual sources of uncertainty X_i	Sub-components Y_j	Symbol	Type
Measured sample signal		V^S_λ	
	Repeatability of FTIR spectrometer measurement	$V^S_{\lambda n}$	A
	Time stability of apparatus	$V^S_{\lambda t}$	B
	Noise of spectral signal	$V^S_{\lambda noise}$	A
	Accuracy of spectrometer wavelength	$V^S_{\lambda \lambda}$	B
	Atmospheric spectral transmission	$V^S_{\lambda at}$	B
	Sample position in the z-axis	$V^S_{\lambda Z}$	B
	Sample surface temperature	$V^S_{\lambda T}$	A
Measured laboratory blackbody signal		V^B_λ	
	Repeatability of FTIR spectrometer measurement	$V^B_{\lambda n}$	A
	Time stability of apparatus	$V^B_{\lambda t}$	B
	Noise of spectral signal	$V^B_{\lambda noise}$	A
	Accuracy of spectrometer wavelength	$V^B_{\lambda \lambda}$	B
	Atmospheric spectral transmission	$V^B_{\lambda at}$	B
Sample surface temperature		T^S	
	Noncontact temperature measurement	T^S_{IR}	B
	Effective emissivity of reference coating	T^S_{ref}	A
	XY sample position	T^S_{XY}	A
	Thickness of reference and analyzed coating	T^S_L	B
	Sample surface temperature fluctuation	T^S_f	A
Laboratory blackbody temperature		T^B	
	Real temperature of cavity	T^B_{real}	B
	Temperature stability of cavity	T^B_{stab}	B
	Spectrometric spot position	T^B_{spot}	B
Surroundings temperature		T^0	
	Temperature measurement accuracy of optical box by thermocouple	T^0_{TC}	B
	Surroundings temperature homogeneity	T^0_{hom}	B
Blackbody effective emissivity		$\hat{\varepsilon}^B$	B
Surroundings emissivity		ε^0	B

4. Methods for particular uncertainties evaluation

In this chapter the detailed evaluation of individual sources of total uncertainty $\mu(X_i)$ and partial uncertainties of sub-components $\xi(Y_j)$ are discussed. The spectral, temperature and angular dependences are not indicated for better readability.

4.1. Uncertainty of the measured signal of the sample

The uncertainty of measured signal of the sample $\mu(V^S_\lambda)$ results from the uncertainty of used instruments, from the uncertainty of measurement conditions and from the uncertainty of sample position and sample surface temperature. The detection system and laser sample heating contribute mainly by the repeatability of FTIR spectrometer measurement, the accuracy of spectrometer wavelength and the noise of spectral signal. Atmospheric spectral transmission and the time stability of apparatus characterize the contribution of the uncertainty of measurement conditions. The uncertainty of sample position presents the inaccurate position of sample to the rotary parabolic mirror (in the z-axis) and the uncertainty of sample surface temperature includes the fluctuation of sample temperature during the measurement of spectral signal and the temperature field homogeneity of the front side of the sample.

The absolute partial uncertainty of repeatability of FTIR spectrometer measurement $\mu(Y_1) = \mu(V^S_{\lambda n})$ was determined as the standard deviation from a measurement series of 20 spectral signals of internal source of spectrometer while the same measurement conditions were maintained. The relative partial uncertainty of the sub-component $\xi(V^S_{\lambda n})$ is related to the average spectral signal from the series of measurements. The absolute and relative uncertainty are only function of wavelength.

The response function of FTIR spectrometer $R_\lambda(\lambda)$ (equation (4) in [20]) describes the time stability of apparatus. Two measurement series of the blackbody spectral signals $V^{B1}_\lambda(\lambda, T^{B1})$ and $V^{B2}_\lambda(\lambda, T^{B2})$ at the temperatures T^{B1} = 300°C and T^{B2} = 900°C were performed in two time intervals t_1 and t_2, and these have been used to calculate of the response functions $R_{\lambda t1}(\lambda)$ and $R_{\lambda t2}(\lambda)$. Between these two measurements, several high-emissivity coatings were analyzed in the temperature range from 300°C to 900°C with temperature step 100°C. The absolute partial uncertainty of time stability of apparatus

$\mu(Y_2) = \mu(V^S_{\lambda t})$ was evaluated as an absolute value of the response functions difference according to equation

$$\mu\left(V^S_{\lambda t}\right) = \left|R_{\lambda t1}(\lambda) - R_{\lambda t2}(\lambda)\right| \ . \tag{5}$$

The relative partial uncertainty $\xi(V^S_{\lambda t})$ is related to the response function $R_{\lambda t2}(\lambda)$. The absolute and relative uncertainty are only function of wavelength.

The similar evaluation as in the uncertainties of repeatability of FTIR spectrometer measurement has been used for absolute and relative partial uncertainties of noise of spectral signal ($\mu(Y_3) = \mu(V^S_{\lambda\ noise})$ and $\xi(V^S_{\lambda\ noise})$). The blackbody spectral signals $V^B{}_\lambda(\lambda, T^B)$ at the temperatures from 300°C to 900°C with temperature step 100°C were detected instead of the spectral signals of internal source of spectrometer. A repeated detection of the blackbody spectral signals has been made for each temperature level. The absolute partial uncertainty of the sub-component $\mu(Y_3)$ was determined as the standard deviation from a measurement series of 20 spectral blackbody signals at the same temperature. The relative partial uncertainty of the sub-component is related to the average spectral signal at the blackbody steady temperature. A spectral and temperature dependence of partial uncertainties was evaluated in this manner.

The uncertainty of accuracy of spectrometer wavelength results from the wave number accuracy specified by the manufacturer of spectrometer. The absolute uncertainty of accuracy of spectrometer wavelength $\mu(Y_4) = \mu(V^S_{\lambda\,\lambda})$ is executed according to

$$\mu\left(V^S_{\lambda\,\lambda}\right) = \frac{10000}{\nu} - \frac{10000}{\nu + \Delta\nu}, \tag{6}$$

where ν is wave number and $\Delta\nu$ is wave number accuracy specified by the manufacturer of spectrometer. The relative uncertainty $\xi(V^S_{\lambda\,\lambda})$ is related to the wavelength. They do not depend on the temperature and radiation angle of analyzed sample.

The uncertainty of atmospheric spectral transmission reflects changes in the atmospheric conditions of measurement between individual calibrations of measuring apparatus. A variation of the concentration of CO_2 and water vapor has been simulated and appropriate spectral signals were detected. The first, a reference spectral signal was measured for the initial setup and the second, spectral signals were recorded for increased concentration of CO_2 and water vapor. In total, five sample spectral signals with controlled atmospheric conditions were analyzed. The absolute partial uncertainty of atmospheric spectral transmission $\mu(Y_5) = \mu(V^S_{\lambda\ at})$ was determined as the standard deviation over all measured spectral signals, the relative partial uncertainty of the sub-component $\xi(V^S_{\lambda\ at})$ is related to the reference spectral signal. The absolute and relative uncertainty are only function of wavelength.

The accurate position of sample to the rotary parabolic mirror (sample position in the z-axis) is assessed by the operator of measuring apparatus according to mutual overlapping of the alignment laser beam. If the laser beams cross each other, the sample measuring position is adjusted. Some inaccuracy of the sample position is always reached. The maximum possible inaccuracy should be used for the evaluation of uncertainty of sample position in the z-axis. The maximum deviation from accurate position was defined as ± 5 mm. Three sample spectral signals at the sample temperature 350°C were detected for three sample distances from the rotary mirror. A reference signal was measured for sample setting in the reference position and other two signals were detected for sample

setting ± 5 mm from the reference position. The absolute partial uncertainty of sample position in the z-axis $\mu(Y_6) = \mu(V^S_{\lambda z})$ was evaluated as the standard deviation of the detected spectral signals. The relative partial uncertainty $\xi(V^S_{\lambda z})$ is related to the reference sample spectral signal.

The calculation of partial uncertainty of sample surface temperature is derived from the fluctuation of sample temperature during the measurement of spectral signal and the temperature field homogeneity of the front side of the sample. The temperature field homogeneity of the sample represents the temperature distribution in area on the sample surface analyzed by the spectrometer (analyzed area). The sample temperature stabilization in the temperature range from 300°C to 900°C with temperature step 100°C was gradually achieved and a temperature matrix of analyzed area was measured by an infrared camera. The spectral radiance computed according to the Planck's law [26, 27] was evaluated for each temperature in analyzed area. A standard deviation of Planck's curves was used and the absolute uncertainty of temperature field homogeneity was determined. The relative uncertainty is related to the spectral radiance computed according to the Planck's law for the average temperature of temperature matrix.

The fluctuation of sample temperature during the measurement of spectral signal means the sample temperature variations in analyzed area during the spectrometric record. The temperatures were measured by an infrared camera and the spectral radiation computed according to the Planck's law was calculated for each temperature. The absolute uncertainty of the fluctuation of sample temperature is evaluated as the standard deviation of the Planck's curves. The relative uncertainty is related to the spectral radiance computed according to the Planck's law for the average temperature from spectrometric record.

The total relative partial uncertainty of sample surface temperature $\xi(Y_7) = \xi(V^S_{\lambda T})$ is computed as the square root of the sum of squares of the relative uncertainty of sample temperature homogeneity and sample temperature fluctuation. The spectral and temperature dependence of sub-component uncertainty is also evaluated.

4.2. Uncertainty of the measured signals of the laboratory blackbody

The uncertainty of the measured signals of the laboratory blackbody $\mu(V^{B1}_{\lambda})$ and $\mu(V^{B2}_{\lambda})$ includes the same sub-components such as the uncertainty of measured signal of the sample. The same method of calculation is also used for their determination. The sub-components of sample position in the z-axis and sample surface temperature are omitted.

4.3. Uncertainty of the sample surface temperature

The main contribution to the total uncertainty of emissivity is the uncertainty of sample surface temperature. Many sub-components (Table 1) determine this uncertainty.

The sample surface temperature is measured noncontactly by the calibrated infrared camera with wavelength range from 7.5 μm to 13 μm. We calibrated the infrared camera against a calibrated blackbody Omega BB-4A in temperature range between 200°C and 1000°C with temperature step of 100°C. The indentified temperature differences of thermography system have been included in the emissivity measurement for more precise determination of analyzed surface temperature. The results of blackbody calibrations (referred uncertainty of calibration and time stability of temperature) were used for the estimation of the partial uncertainty of noncontact temperature measurement. The relative partial uncertainty of noncontact temperature measurement $\xi(Y_1) = \xi(T^S_{IR})$ is computed as the square root of the sum of squares of the relative uncertainties of blackbody calibrations. These are related to the calibrated temperature of blackbody cavity and are only temperature dependent.

Reference ZYP coating Cr_2O_3 with a known temperature dependent effective emissivity for the infrared camera is deposited on the half of sample front side for precise evaluation of the sample surface temperature. The effective emissivity of the coating was analyzed in detail for the different time and temperature regimes. The method is described in detail in [20]. The relative uncertainty of thermocouple temperature measurement accuracy at the interface of reference and analyzed coating in the effective emissivity analysis and relative uncertainty of effective emissivity variance with time duration of the measurement at the temperature level are entering to the computation of partial uncertainty of effective emissivity of reference coating.

A calibrated thermocouple was welded to a coating/substrate interface and a maximum temperature difference of thermocouple measurement including thermocouple temperature contributions had been estimated. In total, three temperatures at the interface of reference and analyzed coating were defined for each temperature level in the temperature range from 300°C to 900°C. The first, a reference temperature was defined for thermocouple's temperature. The other two temperatures corresponded to the reference temperature ± maximum temperature deviation. The effective emissivity of reference coating was evaluated for this three temperatures and the absolute sub-uncertainty was computed as standard deviation of effective emissivities. The relative sub-uncertainty was related to the temperature measured by the thermocouple.

The effective emissivity analysis of reference coating with time duration of the measurement at temperature level was performed. In this experiment, the sample temperature was stabilized to a required value according temperature measured by a thermocouple welded at the coating/substrate interface and a sample temperature filed was detected by the infrared camera. At each temperature level, thirty effective emissivities were analyzed in a time interval of 30 minutes and the average effective emissivity was also computed. The absolute sub-uncertainty was evaluated as the standard deviation from the effective emissivities and the relative sub-uncertainty was related to the average effective emissivity of reference coating.

The total relative partial uncertainty of effective emissivity of reference coating $\xi(Y_2) = \xi(T^S_{ref})$ was computed as the square root of the sum of squares of the relative sub-uncertainties. Only the temperature dependence is determined.

The alignment lasers settings and positioning of thermogram analysis for the evaluation of sample surface temperature also contribute to the uncertainty of sample surface temperature. These contributions are summarized to the sub-component of XY sample position. The analyzed coating was deposited over the entire sample surface and the reference coating was sprayed on half of the area of analyzed coating. A thermogram was recorded after sample temperature stabilization at required temperature level and sample surface temperature distribution was analyzed for each temperature level in the temperature range from 300°C to 900°C with temperature step 100°C. A temperature distribution was evaluated by the different location of analysis on the surface of reference coating. In total, nine temperatures were evaluated as average temperatures from the areas. The initial analysis was placed symmetrically to the area detected by the spectrometer on the part of the sample with a reference coating and other analyses have been successively displaced by ± 1 mm and ± 2 mm in the direction of x and y axes (Fig. 1). The analysis size corresponded to the area detected by the spectrometer. The absolute partial uncertainty of XY sample position $\mu(Y_3) = \mu(T^S_{XY})$ was determined by the standard deviation over all average temperatures at different places. The relative partial uncertainty $\xi(T^S_{XY})$ was related to the temperature obtained from the initial analysis.

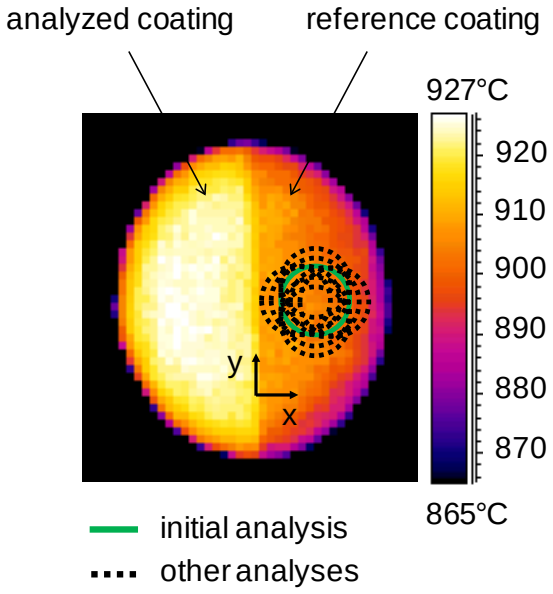

Fig. 1. Thermogram with measuring positions of sample surface temperatures on the reference coating for the uncertainty of XY sample position evaluation.

The radiative properties of the sample are affected by the application of reference and analyzed coating on the substrate. Especially, the different thicknesses of both applied coatings, deposition

repeatability of reference coating and unknown thickness of analyzed coating contribute to the uncertainty of the sample surface temperature. The sensitivity analyses of spectral emissivity measuring method [22] was performed and the results were used to calculate the absolute temperature differences between average temperature on the surface of analyzed coating and average temperatures at the interface of reference and analyzed coating using by an experimental mathematical model [28]. The absolute temperature differences were determined for a wide thickness range of reference and analyzed coatings, different emissivities of analyzed coating and each sample temperature level. All absolute sub-uncertainties were evaluated as the standard deviations of the absolute temperature differences for each temperature level. The relative sub-uncertainties were related to the temperature level. The total relative partial uncertainty of thickness of reference and analyzed coating $\xi(Y_4) = \xi(T^S_L)$ was computed as the square root of the sum of squares of the relative sub-uncertainties at each temperature level.

The sample surface temperature fluctuation is the last sub-component contributing to the uncertainty of sample surface temperature. As in the calculation of partial uncertainty of sample surface temperature in the uncertainty of measured signal of the sample, by the fluctuation is meant the sample temperature variations in analyzed area during the spectrometric record. In this case, the sample was gradually heated to the required temperatures in the temperature range from 300°C to 900°C with temperature step 100°C and sample surface temperature in analyzed area was recorded by the infrared camera during spectrometric measurement. The absolute uncertainty of the sample surface temperature fluctuation $\mu(Y_5) = \mu(T^S_f)$ was determined as the standard deviation of the measured sample surface temperature at each temperature level. The relative uncertainty $\xi(T^S_f)$ is related to the average sample temperature.

4.4. *Uncertainty of the laboratory blackbody temperatures*

The laboratory blackbody was calibrated by Czech Metrology Institute and the calibration uncertainties were determined. Specifically, the difference between required and real temperature of the cavity was evaluated, the temperature stability of cavity and the homogeneity of temperature field have been also defined. The calibration was performed in the temperature range from 150°C to 950°C and the results are applied to determine the uncertainty of laboratory blackbody temperatures.

The difference between required and real temperature of the cavity is included to the setting of required of blackbody temperature. Therefore, the partial uncertainty of real temperature of cavity $\mu(Y_1) = \mu(T^B_{real})$ is consistent with the calibration uncertainty. The relative uncertainty $\xi(T^B_{real})$ is related to the real temperature of blackbody cavity.

Temperature stability of cavity was evaluated as the standard deviation from the temperatures measured by a standard pyrometer for 30 minutes. The absolute partial uncertainty of temperature

stability of cavity $\mu\ (Y_2) = \mu\ (T^B_{stab})$ corresponds to this value. The relative uncertainty $\xi\ (T^B_{stab})$ is related to the real temperature of blackbody cavity again.

The uncertainty of spectrometric spot position indicates the relative position of blackbody and rotary parabolic mirror. The configuration was adjusted so that the maximum blackbody spectral signal was achieved (for each temperature level). The calibration results of the homogeneity of temperature field showed that the temperature distribution of the blackbody cavity is not homogeneous. In the X direction, the maximum temperature corresponds to the centre of blackbody cavity. In the Y direction, the maximum temperature is situated between the cavity center and the cavity upper part. The absolute uncertainty of spectrometric spot position $\mu\ (Y_3) = \mu\ (T^B_{spot})$ was calculated from the blackbody spectral signals by

$$\mu\left(T^B_{spot}\right) = \left|\max\left\{V^B_{\lambda,C}\left(\lambda, T^B\right)\right\} - \max\left\{V^B_{\lambda,TDC}\left(\lambda, T^B\right)\right\}\right|, \tag{7}$$

where $max\{V^B_{\lambda,C}\ (\lambda,\ T^B)\}$ is maximum blackbody spectral signal for the radiation from blackbody cavity centre and $max\{V^B_{\lambda,TDC}\ (\lambda,\ T^B)\}$ is maximum blackbody spectral signal for the radiation from blackbody cavity upper part. The relative uncertainty of spectrometric spot position $\xi\ (T^B_{spot})$ is related to the temperature in the centre of blackbody cavity.

4.5. *Uncertainty of the surroundings temperature*

The optical path from the sample and the blackbody is covered by the optical box. Box temperature is measured by two calibrated thermocouples attached to the inner walls close to the scanning head and in a place between the sample and infrared camera. The second temperature is considered as the surroundings temperature. The box temperature distribution is not measured. Therefore, accuracy of thermocouple temperature measurement and surroundings temperature homogeneity are sub-components of the surroundings temperature uncertainty.

The thermocouple was calibrated and the uncertainty of the calibrator was taken as the absolute partial uncertainty of thermocouple temperature measurement accuracy $\mu\ (Y_1) = \mu\ (T^0_{TC})$. The relative uncertainty $\xi\ (T^0_{TC})$ is related to the actual box temperature measured by the thermocouple.

The box temperature homogeneity was inspected by an infrared camera when the sample was heated in the temperature range from 300°C to 900°C with temperature step 100°C. For each temperature level, the temperature distribution was analyzed, and temperature deviation ΔT^0 and absolute partial uncertainty of surroundings temperature homogeneity $\mu\ (Y_2) = \mu\ (T^0_{hom})$ were evaluated by

$$\mu\left(T^0_{hom}\right) = \Delta T^0 = \left|T^0_{ref} - T^0_{\max}\right|, \tag{8}$$

where T^0_{ref} is thermocouple temperature in place between the sample and infrared camera and T^0_{max} is the maximum temperature of optical box measured by the infrared camera. The relative partial uncertainty $\xi\ (T^0_{hom})$ is related to the temperature deviation T^0_{ref}.

4.6. *Uncertainty of the laboratory blackbody effective emissivity*

The blackbody manufacturer (Omega Engineering) specifies the effective emissivity of blackbody cavity 0.99. Therefore, the blackbody effective emissivity resolution is 0.01. If uniform distribution of a random quantity [29] is assumed, the absolute uncertainty can be counted according to

$$\mu\left(\hat{\varepsilon}^{B}\right)=\frac{resolution}{2\sqrt{3}}=\frac{0.01}{2\sqrt{3}}\ . \tag{9}$$

4.7. *Uncertainty of the surroundings emissivity*

The inner walls of the optical box are painted with high-emissivity coating DupliColor 800°C. The spectral emissivity of the coating at the temperature 100°C was measured in LNE [13] and total hemispherical emissivity has been calculated. The surroundings emissivity is not included in the equation (1) to the computation of spectral emissivity of materials. The absolute uncertainty of surroundings emissivity $\mu\ (\varepsilon^{0})$ is calculated as the difference between the considered surroundings emissivity (ε^{0} = 1) and the real one (ε^{0} = 0.947).

5. Examples of results

As mentioned, the emissivity uncertainty is related to a specific sample. In Fig. 2a, a spectral curve of the coating DupliColor 800°C (MOTIP DUPLI Ltd, Germany) at the temperature 800°C is shown as an example. Also the range of the combined standard uncertainty with coverage factor k = 2 calculated according to equation (2) is shown as $\varepsilon \pm \Delta\varepsilon$. Additionally, the uncertainty is shown as a single curve in Fig. 2b. The emissivity spectrum is affected by changing atmospheric absorption (H_2O and CO_2) in wavelength ranges from 2.5 μm to 2.95 μm, 4.17 μm to 4.5 μm, 4.8 μm to 8 μm and from 13.2 μm to 17.2 μm. In these spectral ranges, the emissivity uncertainty is up to 60%. If the measurements would be done in vacuum, the uncertainty in these bands would be significantly reduced. Except the mentioned atmospheric absorption bands the emissivity uncertainty is lower than 4% in the spectral range up to 19 μm. In the spectral range from 19 μm to 25 μm, the uncertainty gradually increases up to 10%. The spectral emissivity of analyzed coating is between 0.72 and 1 depending on the wavelength. The value 1 is not exceeded. In all bands of the atmospheric absorption and in the band from 17.2 μm to 19.5 μm, the emissivity with emissivity uncertainty exceeds the value 1. The real emissivity value of the coating is of course between the lower limit of uncertainty and one.

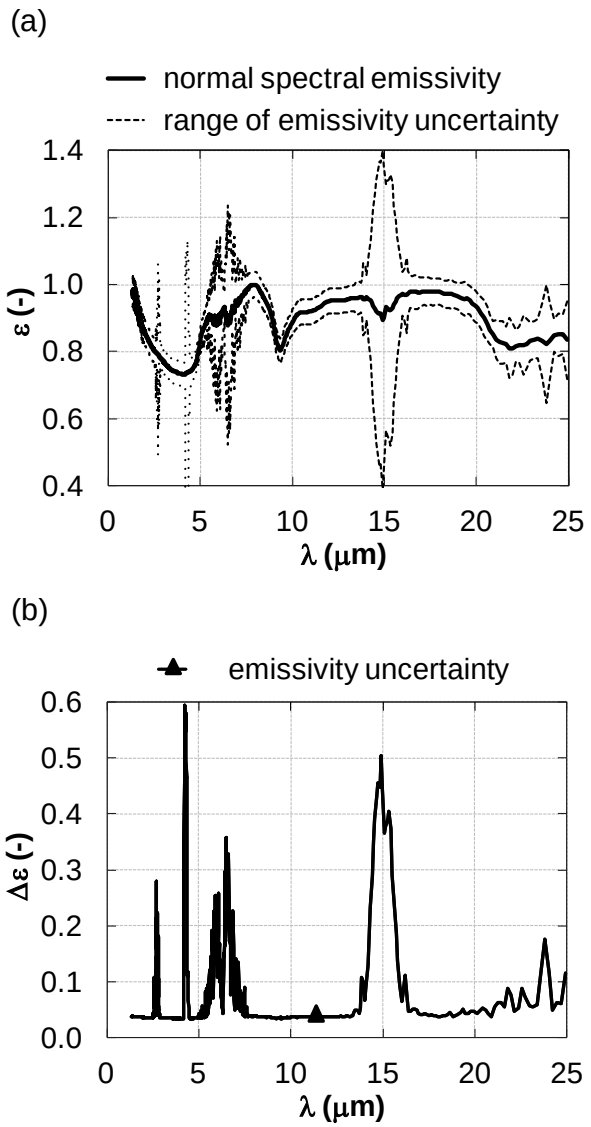

Fig. 2. Example results of normal spectral emissivity and its uncertainty for coating DupliColor 800°C at temperature of 800°C. (a) Spectral normal emissivity with range of expanded emissivity uncertainty (coverage factor k = 2); (b) expanded emissivity uncertainty.

A spectral and temperature dependence of the combined standard uncertainty of emissivity of coating DupliColor 800°C with coverage factor $k = 2$ in the temperature range from 300°C to 900°C and with temperature step 100°C is shown in Fig. 3. Only weak spectral dependence is recognized for all spectral curves. The spectral curves are similar with the curve of emissivity uncertainty indicated in Fig. 2. The uncertainty dependence on temperature is greater than on the wavelength. With increasing the sample surface temperature the emissivity uncertainty increases. The uncertainty is about 2% at the temperature 300°C and is approximately doubled at the temperature 900°C (except the atmospheric absorption bands). Nevertheless, the uncertainty is dominant in the atmospheric absorption bands. Therefore, a detailed evaluation of temperature dependence of combined standard uncertainty has been done for three selected wavelengths 3 μm, 10 μm and 20 μm. The results are shown in Fig. 4.

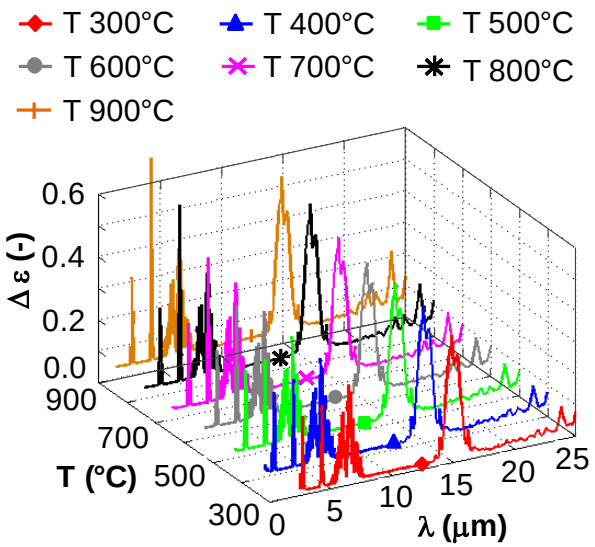

Fig. 3. Spectral and temperature dependence of expanded total uncertainty for emissivity coating DupliColor 800°C.

It is clear from Fig. 4 that the uncertainty significantly depends on the sample surface temperature. With increasing temperature, the uncertainty grows from 2% at sample temperature 300°C or 400°C to 4% at temperature 900°C for the wavelengths 3 μm and 10 μm. The similar temperature dependence is also achieved for the wavelength 20 μm. At the temperature 300°C and 400°C the uncertainty is about 3%, at the temperature 900°C reaches about 5%. The sample surface temperature 600°C is the milestone in the temperature dependence of uncertainty. The uncertainty rapidly grows up to this temperature, above 600°C the growth is slower.

The spectral dependence of combined standard uncertainty is also emphasized in Fig. 4. The lower uncertainty is achieved at shorter wavelengths. With increasing wavelength the emissivity uncertainty increases.

The relative contribution of individual sources to the total uncertainty is shown in Fig. 5 for the emissivity of DupliColor 800°C. The temperature dependence in temperature range from 300°C to 900°C is presented in Fig. 5a for selected wavelength of 10 μm. In analyzed temperature range, the main contribution is due to the sample surface temperature T^S. At 300°C, the contribution is about 35%. With increasing of the sample surface temperature the contribution increases to more than 80% at 600°C. Above the temperature 600°C, the contribution of sample surface temperature is almost constant. Thus, if it is required to increase the emissivity measurement accuracy, more precision temperature measurement is necessary to be provided at higher temperatures. Further, the blackbody effective emissivity $\hat{\varepsilon}^B$ and the measured sample signal V^S_λ contribute significantly to the total uncertainty, especially for the sample temperature lower than 600°C. For example, the contribution of effective emissivity to the total uncertainty is almost 30% at 300°C. The contribution of measured

laboratory blackbody signal $V^{B1}{}_{\lambda}$ at lower temperatures (T^{B1}) is higher than the contribution of laboratory blackbody signal $V^{B2}{}_{\lambda}$ at higher temperatures (T^{B2}). The contribution of $V^{B1}{}_{\lambda}$ is almost independent at the sample temperature and is about 5%. The contribution of surroundings emissivity ε^{0} decreases with increasing temperature from 7% at the temperature 300°C to a negligible value at the temperature 900°C. The contributions of the laboratory blackbody temperatures T^{B1} and T^{B2} and surroundings temperature T^{0} are negligible over the whole temperature range.

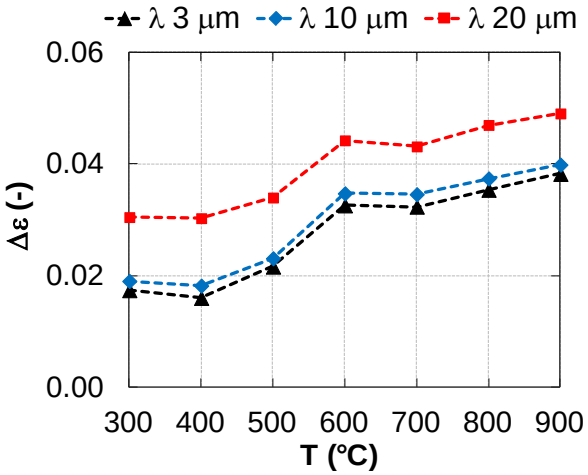

Fig. 4. Temperature dependence of expanded emissivity uncertainty (coverage factor k = 2) for coating DupliColor 800°C at wavelengths 3 μm, 10 μm and 20 μm.

For selected temperature of 800°C, the spectral dependence of the relative contribution of individual sources to the total uncertainty is shown in Fig. 5b. In atmospheric absorption bands (2.5 μm to 2.95 μm, 4.17 μm to 4.5 μm, 4.8 μm to 8 μm and from 13.2 μm to 17.2 μm), the contributions of measured sample signal $V^{S}{}_{\lambda}$ and laboratory blackbody signal $V^{B1}{}_{\lambda}$ are dominant. The other contributions are negligible. Except the mentioned atmospheric absorption bands, the contribution of sample surface temperature T^{S} prevails over the other contributions up to wavelength 20 μm. The contribution is almost 90% of the total uncertainty. For wavelengths above 20 μm, the contribution T^{S} gradually decreases to 20% and the contribution of laboratory blackbody signal $V^{B1}{}_{\lambda}$ becomes dominant in the total uncertainty of emissivity. The contribution of measured sample signal $V^{S}{}_{\lambda}$ is also significant at long wavelengths. The contribution of blackbody effective emissivity $\hat{\varepsilon}^{B}$ is almost independent at wavelengths, it is up to 5%. The contributions of laboratory blackbody temperatures T^{B1} and T^{B2}, surroundings temperature T^{0} and surroundings emissivity ε^{0} are negligible in the analyzed spectral range and selected temperature.

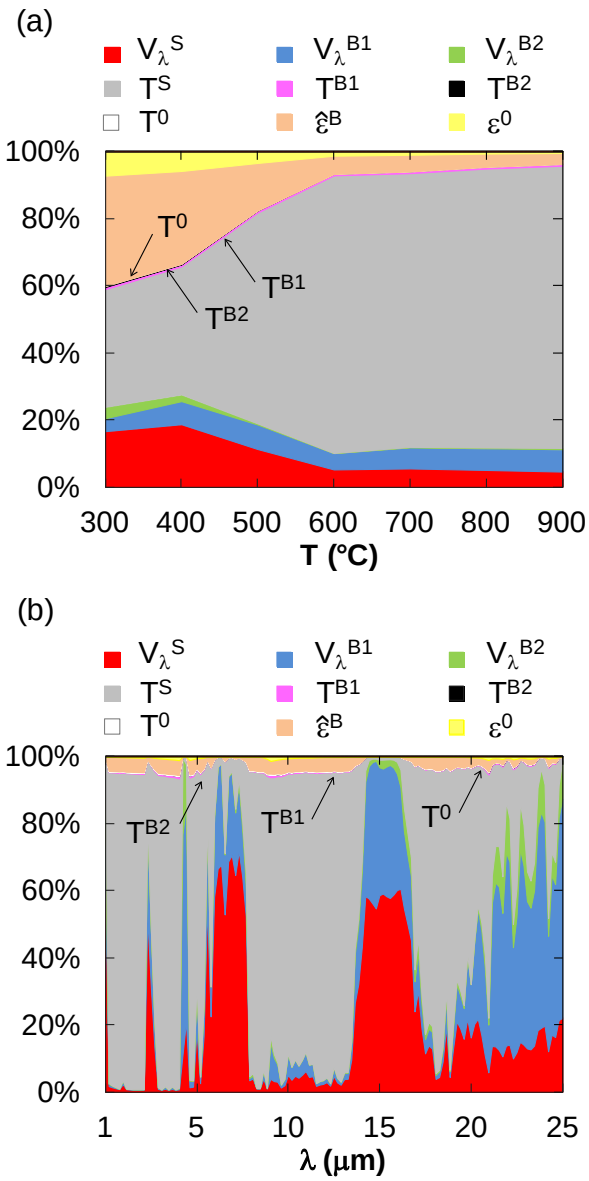

Fig. 5. Relative contribution of each individual uncertainty sources to the total uncertainty for the emissivity coating DupliColor 800°C. (a) Temperature dependence for wavelength 10 μm; (b) spectral dependence for temperature 800°C.

Any individual sources of uncertainty include further sub-components, which contribute to the partial uncertainty of individual sources. These are the measured sample signal V^S_λ, the laboratory blackbody signals V^{B1}_λ and V^{B2}_λ, the sample surface temperature T^S, the laboratory blackbody temperatures T^{B1} and T^{B2} and surroundings temperature T^0. The relative contribution of sub-components to partial uncertainty of individual sources is shown in Fig. 6 as a function of the temperature for the selected wavelength of 10 μm.

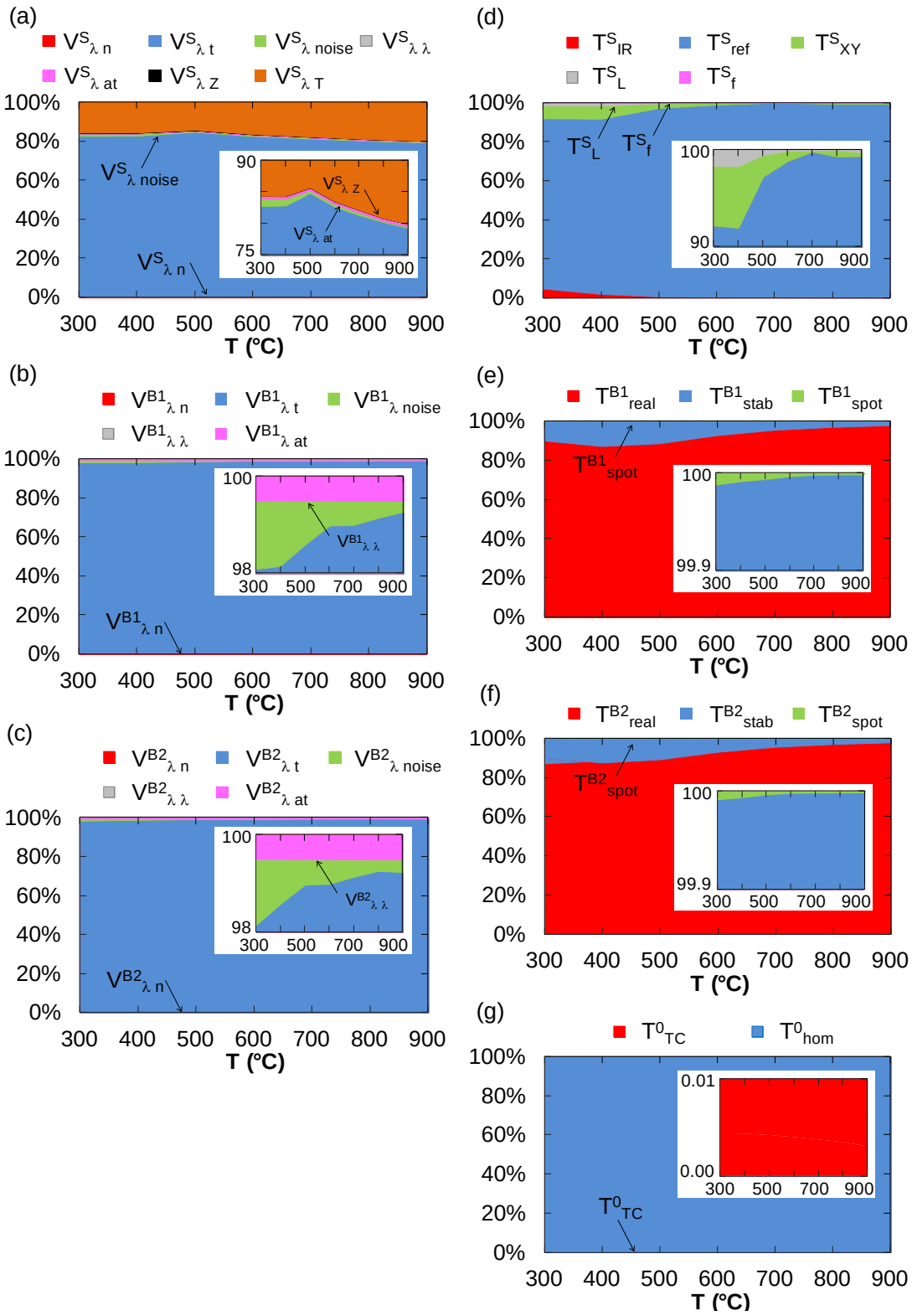

Fig. 6. Relative contribution of sub-components to the partial uncertainty of emissivity of individual sources. Uncertainty of individual source for (a) measured sample signal; (b) laboratory blackbody signal at temperature T^{B1}; (c) laboratory blackbody signal at temperature T^{B2}; (d) sample surface temperature; (e) laboratory blackbody temperature T^{B1}; (f) laboratory blackbody temperature T^{B2}; (g) surroundings temperature.

In the case of partial uncertainty of the measured sample signal V^{S}_{λ} (Fig. 6a), the main sub-components are the time stability of apparatus $V^{S}_{\lambda t}$ (more than 80%) and the sample surface temperature distribution V^{S}_{T} (up to 20%). The other contributions are in the order of several % and these are negligible compared with the above. Only weak temperature dependence of sub-components is observed.

The time stability of apparatus $V^{B}_{\lambda t}$ has almost 100 % portion in the partial uncertainty of laboratory blackbody signals V^{B1}_{λ} and V^{B2}_{λ} (Fig. 6b, 6c). Noise of spectral signal $V^{B}_{\lambda noise}$ and atmospheric spectral transmission $V^{B}_{\lambda at}$ contribute in the order of several %. The noise of spectral signal contributes mainly for lower sample surface temperatures, this decreases with increasing temperature. The atmospheric spectral transmission does not show temperature dependence. The other sub-components contribute by slight fraction.

The effective emissivity of reference coating T^{S}_{ref} is the main contribution in the partial uncertainty of sample surface temperature (Fig. 6d). For the temperature 300°C, the contribution T^{S}_{ref} is around 85%. With increasing the sample surface temperature the contribution increases to 100% at the temperature 600°C. Above the temperature 600°C, the contribution is constant. The other sub-components also influence the partial uncertainty of sample surface temperature especially in lower sample temperature range. The noncontact temperature measurement T^{S}_{IR}, the XY sample position T^{S}_{XY} and the thickness of reference and analyzed coating T^{S}_{L} contribute in order of %. These decreases with increasing sample surface temperature. The contribution of sample surface temperature fluctuation T^{S}_{f} is negligible.

The main sub-components in the partial uncertainty of laboratory blackbody temperatures (Fig. 6e, 6f) are the real temperature of blackbody cavity T^{B}_{real} and the temperature stability of blackbody cavity T^{B}_{stab}. The real temperature of cavity contributes more than 80%, the temperature stability of cavity completes to 100%. For lower temperatures (500°C), the fraction of sub-component T^{B}_{stab} is almost 20%, this decreases with increasing temperature to the several %. The last sub-component (spectrometric spot position T^{B}_{spot}) is only hundredths of % and it is negligible.

Only two sub-components are included to the partial uncertainty of surroundings temperature T^{0} (Fig. 6g) – thermocouple temperature measurement accuracy T^{0}_{TC} and surroundings temperature homogeneity T^{0}_{hom}. The second contributes almost 100% to the analyzed partial uncertainty without temperature dependence.

Each partial uncertainty of individual source has one sub-component which significantly exceeds the other sub-components. The time stability of apparatus $V_{\lambda t}$ is main contribution in the case of the partial uncertainty of measured sample signal and the partial uncertainty of laboratory blackbody signals. The partial uncertainty of sample surface temperature is mostly affected by the effective emissivity of reference coating T^{S}_{ref}. To the partial uncertainty of laboratory blackbody temperatures contributes the most the real temperature of blackbody cavity T^{B}_{real}. The surroundings temperature

homogeneity T^{0}_{hom} is the top contribution to the partial uncertainty of surroundings temperature. The emissivity measurement accuracy could be improved by reducing the contribution of the above sub-components, mainly the effective emissivity of the reference coating.

6. Conclusion

The paper deals with uncertainty analyses of the new laboratory method for the measurement of spectral emissivity of high-temperature coatings. The uncertainty is always related to individual sample being measured. DupliColor 800°C paint (MOTIP Dupli Ltd.) is used as an example to introduce the uncertainty spectral and temperature dependences and to show influence of individual uncertainty sources and their sub-components.

Wavelength distribution of the total uncertainty is strongly affected by atmospheric absorption. Therefore, in the ranges 2.5 – 2.95 μm, 4.17 – 4.5 μm, 4.8 – 8 μm and 13.2 – 17.2 μm the uncertainty is high. Except the absorption bands the uncertainty is below 4 % (coverage factor k = 2) with only weak dependence on the wavelength. Temperature dependence of the total uncertainty is increasing with increasing sample temperature. The uncertainty is about 2% at 300°C, at 900°C the value is two times higher.

Sample surface temperature is the most important parameter concerning its contribution to the total uncertainty. At 300°C its contribution is about 20%. With increasing temperature its contribution is increasing, at 600°C it covers more than 80%. Above the temperature 600°C, the contribution of sample surface temperature is almost constant. Below 600°C the blackbody effective emissivity and measured sample signal considerably contribute to the total uncertainty. For example, the contribution of effective emissivity to the total uncertainty is almost 30% at 300°C. The contribution of measured laboratory blackbody signal is almost independent on the sample temperature and is about 5%. The contribution of surroundings emissivity decreases with increasing temperature from 7% at 300°C to a negligible value at 900°C. The contributions of laboratory blackbody temperatures and surroundings temperature are negligible over the whole temperature range.

The effective emissivity of reference coating is the main contribution in the partial uncertainty of sample surface temperature. For the temperature 300°C, its contribution is about 85%. With increasing sample surface temperature the contribution increases to 100% at 600°C. Above the temperature 600°C, the contribution is constant. The other sub-components also influence the partial uncertainty of sample surface temperature especially in lower sample temperature range. The noncontact temperature measurement, the XY sample position and the thickness of reference and analyzed coating contribute in order of units of %. These decreases with increasing sample surface temperature. The contribution of sample surface temperature fluctuation is negligible.

Acknowledgments

The result was developed within the CENTEM project, reg. no. CZ.1.05/2.1.00/03.0088, cofunded by the ERDF as part of the Ministry of Education, Youth and Sports OP RDI programme and, in the follow-up sustainability stage, supported through CENTEM PLUS (LO1402) by financial means from the Ministry of Education, Youth and Sports under the ”National Sustainability Programme I”.

References

[1] A. Emadi, A. Saboonchi, M. Taheri, S. Hassanpour. *Heating characteristics of billet in a walking hearth type reheating furnace*. Applied Thermal Engineering, Vol. 63, pp. 396-405, 2014.

[2] J. Obando, Y. Cadavid, A. Amell. *Theoretical, experimental and numerical study of infrared radiation heat transfer in a drying furnace*. Applied Thermal Engineering, Vol. 90, pp. 395-402, 2015.

[3] M. Švantner, P. Honnerová, Z. Veselý. *The influence of furnace wall emissivity on steel charge heating*. Infrared Physics and Technology, Vol. 74, pp. 63-71, 2016.

[4] Q. Yin, W. Du, X. Ji, L. Cheng. *Optimization design and economic analyses of heat recovery exchangers on rotary kilns*. Applied Energy, Vol. 180, pp. 743-756, 2016.

[5] S. D. Khivsara, V. Srinivasan, P. Dutta. *Radiative heating of supercritical carbon dioxide flowing through tubes*. Applied Thermal Engineering, 2016, In press, DOI: 10.1016/j.applthermaleng.2016.05.049

[6] W. Yang, A. Fan, J. Wan, W. Liu. *Effect of external surface emissivity on flame-splitting limit in a micro cavity-combustor*. Applied Thermal Engineering, Vol. 83, pp. 8-15, 2015.

[7] T. Echániz, I. Setién-Fernández, R. B. Pérez-Sáez, C. Prieto, R. Escobar Galindo, M. J. Tello. *Importance of spectral emissivity measurements at working temperature to determine the efficiency of a solar selective coating*. Solar Energy Materials and Solar Cells, Vol. 140, pp. 249-252, 2015.

[8] T. Echániz, R. B. Pérez-Sáez, E. Risueno, L. González-Fernández, A. Faik, J. Rodríguez-Aseguinolaza, P. Blanco-Rodríguez, S. Doppiu, M. J. Tello. *Thermal emissivity spectra and structural phase transitions of the eutectic Mg-51%Zn alloy: A candidate for thermal energy storage*. Journal of Alloys and Compounds, Vol. 684, pp. 62-67, 2016.

[9] C. Hemmer, G. Polidori, C. Popa. *Temperature optimization of an electric heater by emissivity variation of heating elements*. Case Studies in Thermal Engineering, Vol. 4, pp. 187-192, 2014.

[10] P. Honnerová, M. Honner. *Survey of emissivity measurement by radiometric methods*. Applied Optics, Vol. 54, pp. 669-683, 2015.

[11] H. Watanabe, J. Ishii, H. Wakabayashi, T. Kumano, L. Hanssen. *Chapter 9 - Spectral emissivity measurements.* Experimental Methods in the Physical Sciences, Vol. 46, pp. 333-366, 2014.

[12] R. B. Pérez-Sáez, L. del Campo, M. J. Tello. *Analysis of the accuracy of methods for the direct measurement of emissivity.* Int. J. Thermophys., Vol. 29, pp. 1141–1155, 2008.

[13] J. Hameury. *Determination of uncertainties for emisivity measurements in the temperature range 200-800°C*. High Temperature High Pressure, Vol. 30, pp. 223-228, 1998.

[14] M. J. Ballico, T. P. Jones. *Novel experimental technique for measuring high-temperature spectral emissivities.* Appl. Spectros., Vol. 49, pp. 335–341, 1995.

[15] L. del Campo, R. B. Pérez-Sáez, X. Esquisabel, I. Fernández, M. J. Tello. *New experimental device for infrared spectral directional emissivity measurements in a controlled environment.* Rev. Sci. Instrum., Vol. 77, 113111 (8 p.), 2006.

[16] C. P. Cagran, L. M. Hanssen, M. Noorma, A. V. Gura, S. N. Mekhontsev. *Temperature-resolved infrared spectral emisivity of SiC and Pt-10 for temperatures up to 900°C.* Int. J. Thermophys., Vol. 28, pp. 581–597, 2007.

[17] Ch. Monte, J. Hollandt. *The determination of the uncertainties of spectral emissivity measurements in air at the PTB.* Metrologia, Vol. 47, pp. 172–181, 2010.

[18] R. Brandt, C. Bird, G. Neuer. *Emissivity reference paints for high temperature applications.* Measurement, Vol. 41, pp. 731–736, 2008.

[19] T. Fu, M. Duan, J. Tang, C. Shi. *Measurment of the directional spectral emissivity based on a radiation heating source with alternating spectral distributions.* International Journal of Heat and Mass Transfer, Vol. 90, pp. 1207-1213, 2015.

[20] P. Honnerová, J. Martan, M. Kučera, M. Honner, J. Hameury. *New experimental device for high-temperature normal spectral emissivity measurements of coatings*. Measurement Science and Technology, Vol. 25, 095501 (9 p.), 2014.

[21] M. Honner, P. Honnerová, M. Kučera, J. Martan. *Laser Scanning Heating Method for High-Temperature Spectral Emissivity Analyses*. Applied Thermal Engineering, Vol. 94, pp. 76-81, 2016.

[22] Z. Veselý, P. Honnerová, J. Martan, M. Honner. *Sensitivity analysis of high temperature spectral emissivity measurement method*. Infrared Physics and Technology, Vol. 71, pp. 217-222, 2015.

[23] EA-4/02 1999 Evaluation of the uncertainty of measurement in calibration European co-operation for accreditation

[24] G. Genta. *Methods for Uncertainty Evaluation in Measurement.* Saarbrücken: VDM Verlag Dr. Müller, 2010, 132 p.

[25] I. Lira. *Evaluating the Measurement Uncertainty: Fundamentals and Practical Guidance.* London: CRC Press, 2002, 251 p.

[26] R. Siegel, J. Howel. *Thermal Radiation Heat Transfer.* Washington: Taylor & Francis, 2001, 864 p.

[27] D. P. DeWitt, G.D. Nutter. *Theory and Practice of Radiation Thermometry.* New York: John Wiley, 1988, 1152 p.

[28] P. Honnerová, Z. Veselý, M. Honner. *Experimental mathematical model as a generalization of sensitivity analysis of high temperature spectral emissivity measurement method.* Measurement, sent for examination.

[29] R. Durrett. *Probability: Theory and Examples.* Cambridge: Cambridge University Press, 2010, 440 p.